Composites Science and Technology **27** (1986) 25–41

Buckling of a Fiber Bundle Embedded in Epoxy

H. T. Hahn and M. M. Sohi

Washington University in St. Louis, School of Engineering and Applied Science, Center for Composite Research, Campus Box 1087, St. Louis, Missouri 63130 (USA)

SUMMARY

Buckling of a fiber bundle embedded in epoxy resin was studied to gain insight into compressive failure mechanisms in unidirectional composites. The fibers used were E-glass, T300 graphite, T700 graphite, and P75 graphite. These fibers were combined with two different resins: Epon 815/V140 and Epon 828/Z. In both resins the failure mode of the bundle was found to be microbuckling of fibers for the first three types of fibers; however, the high-modulus P75 fibers failed in shear without any sign of microbuckling. The strains at which microbuckling occurred were higher than the compressive failure strains of the corresponding unidirectional composites. In the soft resin, Epon 815/V140, fibers buckled at lower strains than in the stiff resin, Epon 828/Z. The buckling strains and the segment lengths followed the trends predicted for a single filament embedded in an infinite matrix.

INTRODUCTION

The recent work by Williams and Rhodes[1] has shown that higher impact resistance can be obtained for composites by using tougher resins because tougher resins can absorb more energy and localize impact damage. However, higher toughness in a resin frequently necessitates a sacrifice of modulus, and a lower modulus may lead to a lower compressive strength for the composite. Therefore, a judicious selection of resin should be based on a balanced evaluation of both impact resistance and compressive strength.

Composites Science and Technology 0266-3538/86/$03·50

The subject of compressive behavior of composites has frequently been addressed in the literature. Although compressive failure of fibers[2] and longitudinal splitting due to tensile radial stress[3] have also been suggested as possible mechanisms triggering failure of unidirectional composites under compression, failure of state-of-the-art structural composites is now believed to be due to microbuckling or kinking of fibers.[4-8]

Monitoring of failure processes in composites is difficult because failure is quite sudden without much warning. Also, the dynamic nature of the final failure makes it difficult to identify the microscopic failure sequence. Therefore, it is necessary to develop a means of containing failure if the failure sequence is to be delineated.

Failure of fibers by themselves under compression was studied by Hawthorne and Teghtsoonian[9] by embedding a single filament in a resin block. They showed that carbon fibers with compressive failure strains of less than about 2% failed due to either shearing or buckling of fibrils. However, no failure was observed in PAN type II and type A fibers up to 3% strain. Thus, pure compressive failure of fibers in structural graphite/epoxy composites is ruled out; yet their failure mechanisms still need to be elucidated. Also, the role of the matrix should be clearly delineated not to overly compromise compressive strength in favor of impact resistance.

In the present work a fiber bundle embedded in epoxy resin was used to contain failure. A bundle of fibers rather than a single fiber was chosen to simulate the fiber–fiber interaction present in real composites. Also, the use of a bundle allowed for fiber failure to be detected by measuring strain, eliminating the tedious task of continuous visual monitoring required during testing of single-filament specimens. The bundle failure detected by strain measurements was nevertheless confirmed by direct examinations of the failed specimens on an optical microscope during and after testing. The effect of matrix properties was investigated using two resins of different stiffnesses.

EXPERIMENTAL PROCEDURE

Four different fibers were combined with two different epoxy resins. Epon 815/V140 was chosen to represent a soft resin, and Epon 828/Z, a stiff resin. Their nominal properties are listed in Tables 1 and 2. Of the fibers chosen, the E-glass fiber bundle contained about 200 filaments, while

TABLE 1
Resin Properties

Epoxy	*Modulus (GPa)*	*Ultimate tensile stress (MPa)*	*Tensile failure strain (%)*
Epon 828/Z (80/20)	3·45	85·4	9
Epon 815/V140 (60/40)	2·13	45·5	14

T300 and T700 graphite fiber bundles had 3000 and 4500 filaments, respectively. There were 2000 filaments in a P75 graphite bundle. The resin properties were measured but the fiber properties were taken from manufacturers' data sheets. Further details of resin formulations and fabrication procedures can be found in Ref. 10.

The IITRI compression fixture was used with a gage length of 13 mm. Specimen thickness varied from 4 to 6·5 mm while the width was kept at 6·5 mm. An Instron testing machine was used at a crosshead speed of 1·3 mm min^{-1}. During testing the fiber bundle was monitored for failure through a Zeiss stereo microscope at magnifications up to 50 ×. Since the fiber bundle occupied a small fraction of the specimen volume, bundle failure did not lead to specimen failure. Thus, bundle failure could be contained and monitored.

The bundle failure was also monitored on stress–strain curves. Two specimens of each material combination had a strain gage attached. Buckling of the bundle always resulted in a sudden stress drop. However, shear failure of the P75 fibers did not.

After bundle failure the specimen was cracked open through the bundle and examined in a scanning electron microscope (SEM). Modes of fiber fracture were noted, and the lengths of broken segments were measured.

TABLE 2
Fiber Properties

Fiber	*Diameter (μm)*	*Cross-sectional area of bundle (mm^2)*	*Modulus (GPa)*	*Tensile failure strain (%)*
E-Gl	13·5	$2{\cdot}92 \times 10^{-2}$	72·35	4·8
T700	5·1	$9{\cdot}16 \times 10^{-2}$	234·00	1·83
T300	7·0	$11{\cdot}61 \times 10^{-2}$	230·00	1·34
P75	9·7	$14{\cdot}84 \times 10^{-2}$	517·00	0·40

RESULTS AND DISCUSSION

Failure modes

Figure 1 shows buckling of the E-glass bundle in a weak epoxy over its entire length. The epoxy, Epon 815/V140, had too much solvent inadvertently added during formulation, and as a result was much softer than it should have been. Buckling of the fiber bundle in this epoxy was quite gradual, starting at a very low load, and occurred uniformly over the entire gage length.

The elliptical spots on the bundle are cracks growing into the matrix almost normal to the plane of the photograph. These cracks were generated by the tensile stress between fibers as a result of buckling. Note also that fibers have not yet broken even though they are bent.

Buckling of the E-glass bundle in a well-formulated Epon 815 is catastrophic and quite localized (Fig. 2). Buckling occurs without warning and immediately leads to fracture of fibers. Fiber fracture is seen to progress from one edge of the bundle to the other.

Buckling of the E-glass bundle in the stiffer Epon 828 is also quite localized (Fig. 3). Although the bundle has an elliptical cross-section, it can buckle in the plane of the larger dimension as well. The buckled region is out of focus because of the out-of-plane movement of the bundle.

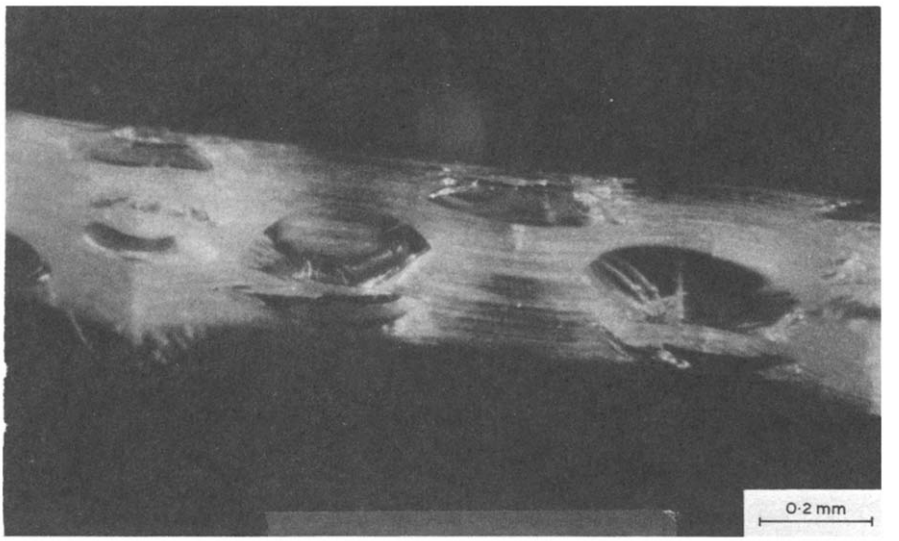

Fig. 1. Uniform buckling of E-glass bundle in a weak Epon 815/V140.

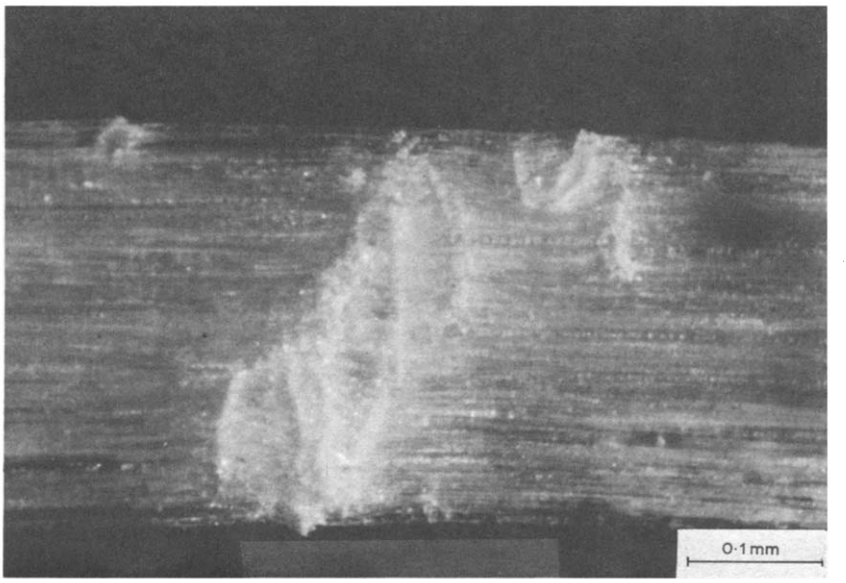

Fig. 2. Localized buckling of E-glass bundle in Epon 815/V140.

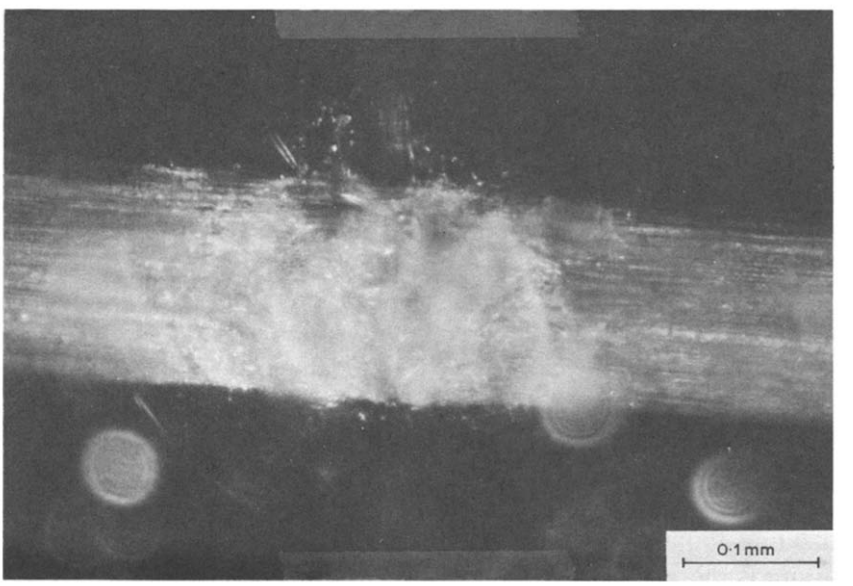

Fig. 3. Localized buckling of E-glass bundle in Epon 828/Z.

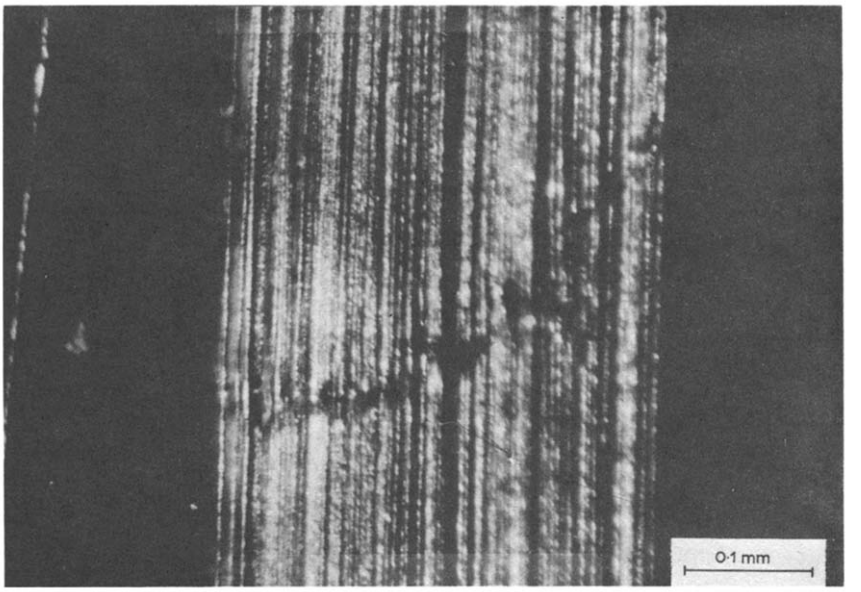

Fig. 4. Localized failure of T300 graphite bundle in Epon 828/Z.

Macroscopically, no distinction could be detected between Epon 815 and Epon 828.

Failure of the T300 graphite fiber bundle in Epon 815 is similar to that of the E-glass bundle in Epon 828. However, the failure zone of the T300 bundle in Epon 828 is much narrower. Also, there is very little indication of failure of the bundle in Epon 828. Rather, only a thin dark line indicates failure of the bundle (Fig. 4).

The high-strain T700 graphite behaves in a similar way to the T300 graphite; the failure is localized and Epon 828 results in a smaller failure zone than Epon 815.

After compression tests, one specimen from each group was cracked open along the bundle. The SEM micrographs of E-glass bundles clearly show a buckling-induced failure (Fig. 5); the broken fiber segments are seen to have rotated and the broken ends are square. Buckling is over a distance of several wavelengths. Very little difference was seen between the two resins.

As mentioned earlier, the T300 graphite bundle shows more localized buckling failure than does the E-glass bundle (Fig. 6). Furthermore, failure is more of a kinking type; that is, fibers are broken at only two locations. Such behavior is not surprising for the following reasons. As in

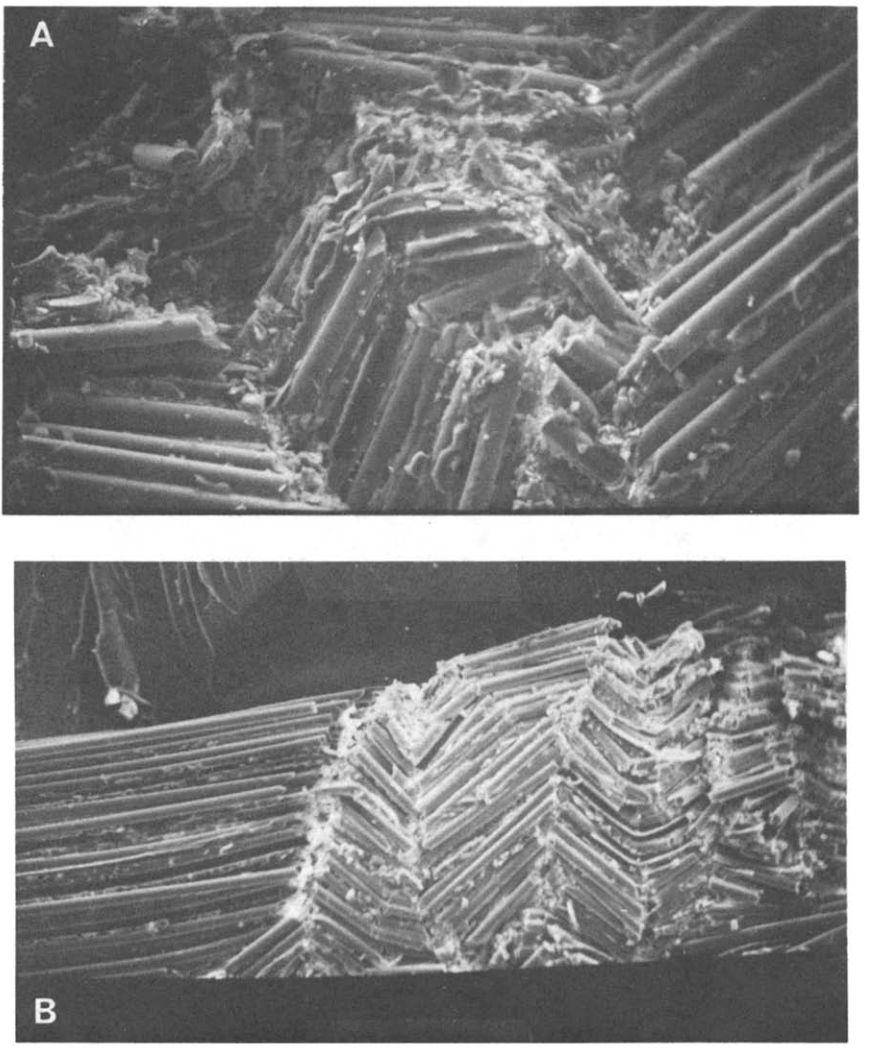

Fig. 5. SEM micrographs of E-glass bundles: (A) Epon 815/V140; (B) Epon 828/Z.

tension, buckling will occur first at the weakest point. If fiber fracture does not follow immediately, buckling will spread along the fiber axis. Since graphite fibers have lower tensile failure strain than glass fibers, the former are more likely to fail immediately after buckling. This may explain why the kinking type of failure is observed in the graphite bundles.

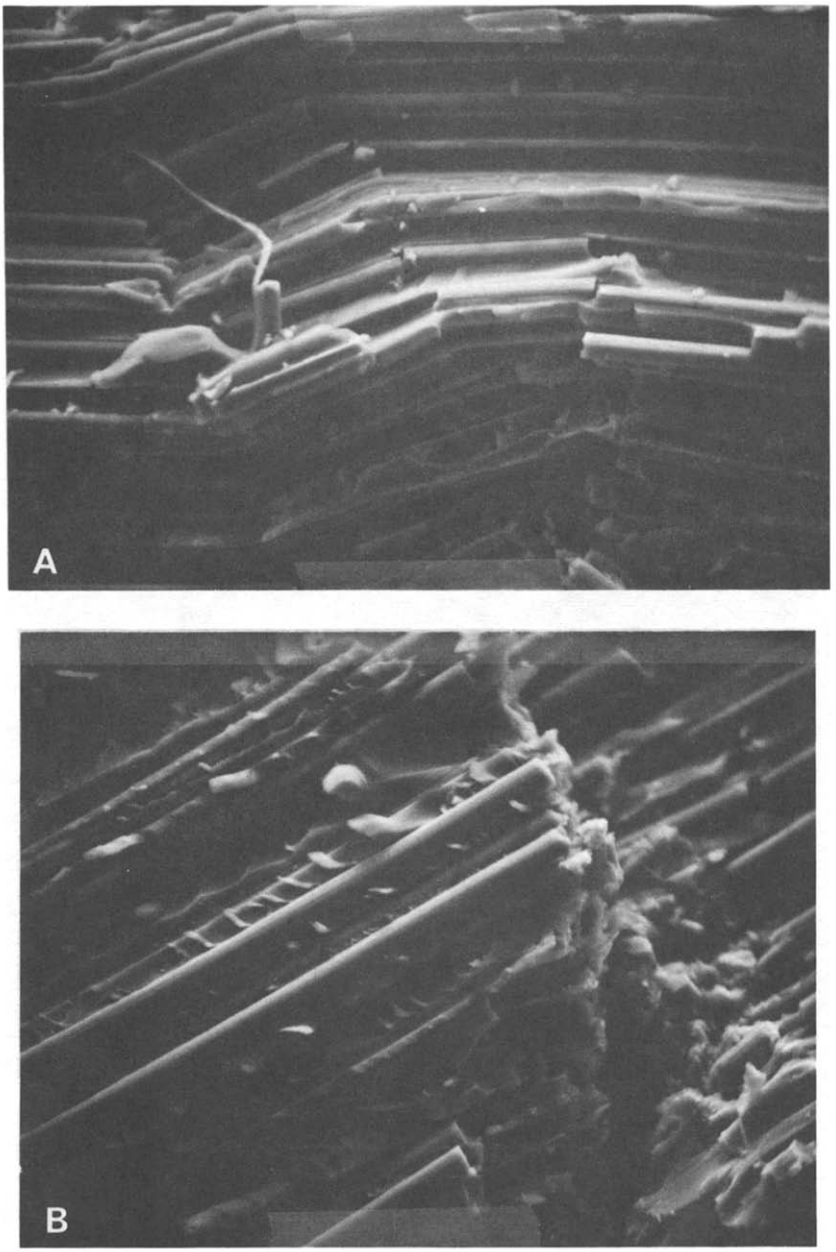

Fig. 6. SEM micrographs of T300 graphite bundles: (A) Epon 815/V140; (B) Epon 828/Z.

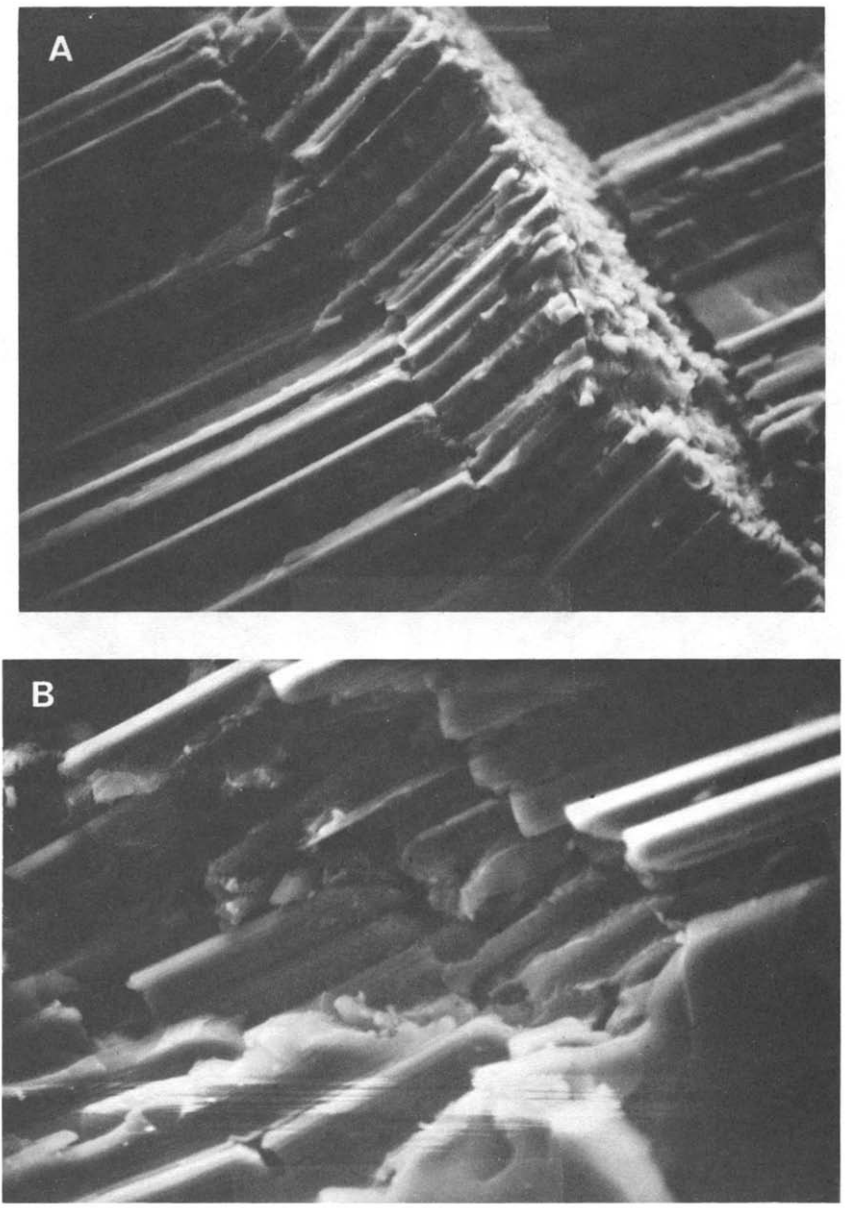

Fig. 7. SEM micrographs of T700 graphite bundles: (A) Epon 815/V140; (B) Epon 828/Z.

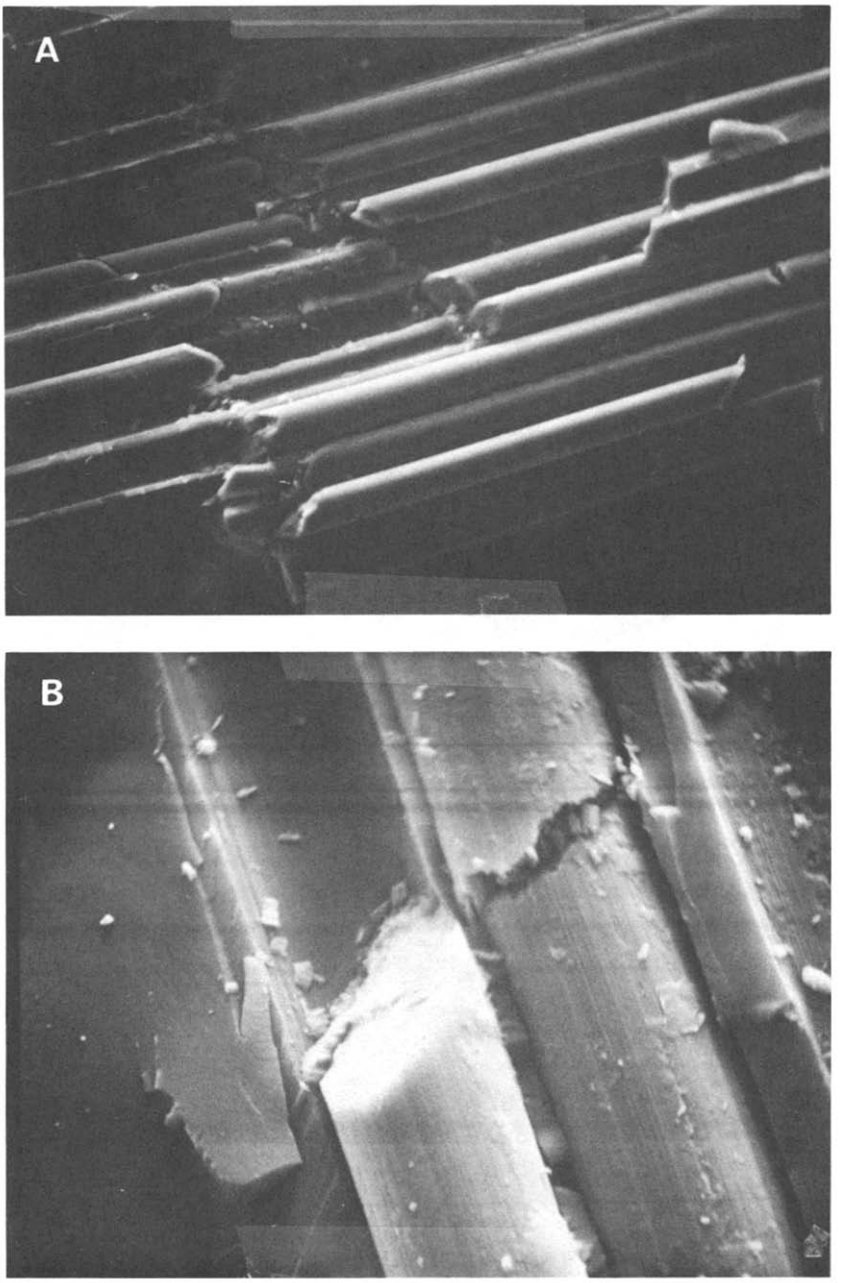

Fig. 8. SEM micrographs of P75 graphite bundles: (A) Epon 815/V140; (B) Epon 828/Z.

The failure modes of T700 fibers observed in SEM micrographs are similar to those of T300 fibers (Fig. 7).

The high-modulus P75 fibers failed in shear without buckling; slanted fracture surfaces are seen in Fig. 8. Even after failure the fibers remain straight without rotation or curvature. A closer examination of the fracture surfaces reveals that the failure of P75 fibers is really due to kinking of fibrils (Fig. 8(b)). It should be noted that the P75 fibers have a highly oriented structure and thus behave like a unidirectional composite on a microscopic scale.

The shear failure of P75 fibers was quite uniformly distributed over the entire length, whereas the buckling failure of the other fibers was only at a few isolated sites along the bundle. In other words, the compressive failure of P75 fibers is more like the multiple fractures that are frequently observed in the tensile testing of fibers embedded in resin.

The number of fiber breaks and the average length of each segment in a failure zone are shown in Fig. 9. The geometrical details of the failure zone vary much more than could be described by average numbers alone. Yet the data in the figure indicate a definite trend.

As was seen earlier, the failure mode of P75 fibers is a single, slanted fracture surface. The failure of T700 fibers in both epoxies and T300 fibers in Epon 828 is characterized by double breaks in each filament, i.e. fiber kinking. The number of breaks increases to three for the T300 fibers in Epon 815. The E-glass bundle exhibits more than three breaks in each

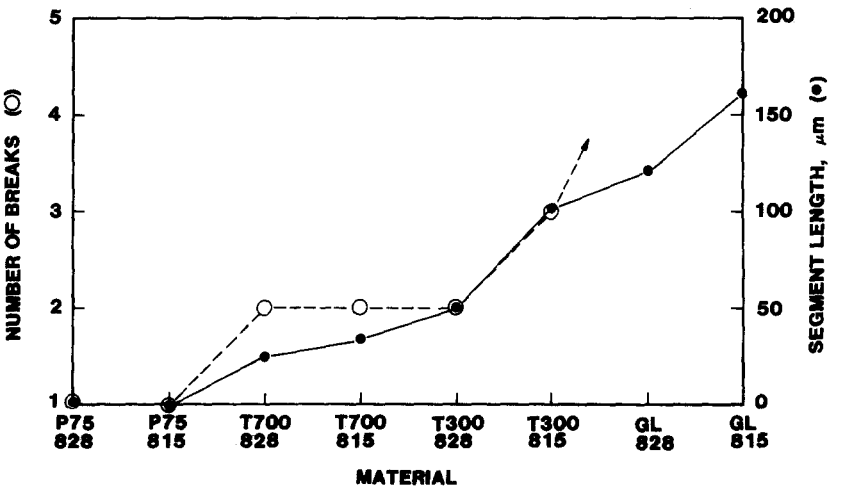

Fig. 9. Number of fiber breaks and average segment lengths.

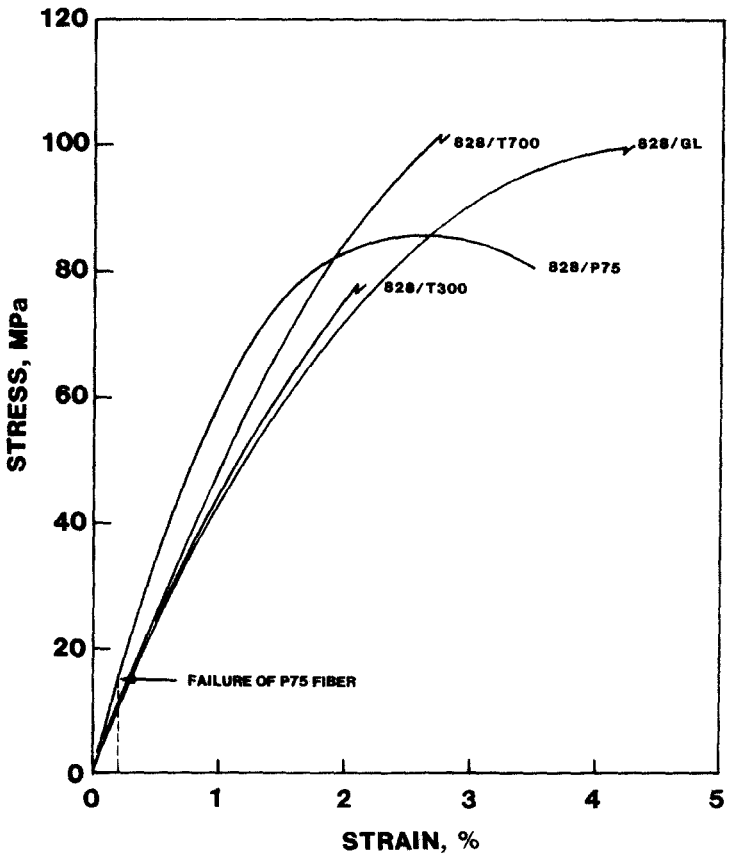

Fig. 10. Stress–strain curves for Epon 828/Z specimens with embedded fiber bundles.

filament regardless of the epoxy type. The length of each segment also increases with the number of breaks.

Failure strains

Typical stress–strain curves for Epon 828 specimens are shown in Fig. 10, where buckling of the bundle is seen to occur when the resin is in the nonlinear range. Since the average fiber volume content is in the order of 0·4%, fibers do not greatly affect the initial modulus: the rule-of-mixtures predictions based on the properties of Tables 1 and 2 are 3·6 GPa for E-glass, 4·2 GPa for T300 and T700 graphite, and 5·5 GPa for P75 graphite. Similar stress–strain relations but with lower moduli were obtained for Epon 815.

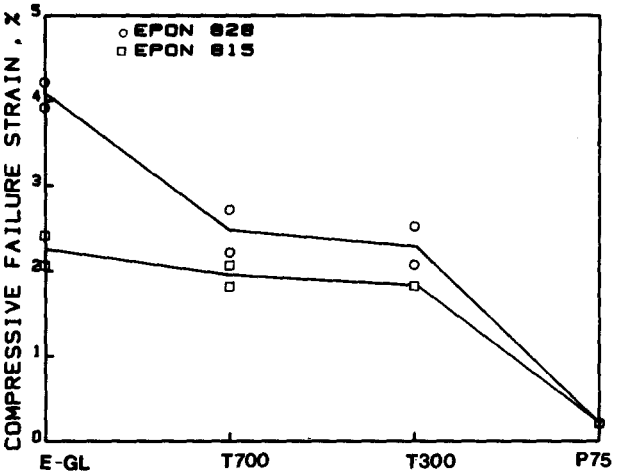

Fig. 11. Compressive failure strains of bundles.

As mentioned earlier, the failure of P75 fibers did not result in a sudden drop in stress (Fig. 10). Rather, the tangent modulus changed only slightly. The change was more distinctive in Epon 815 than in Epon 828 because the former resin was softer.

The measured compressive strains at failure are shown in Fig. 11. The E-glass fiber bundle is seen to have the highest failure strain while the P75 bundle has the lowest. The high-strain T700 graphite bundle is slightly stronger than the T300. As expected from the buckling theory, the stiffer epoxy yields higher failure strains. However, the difference for the T300 and T700 graphite fibers is much less than for the E-glass, and disappears for the P75. Since the failure of P75 fibers is in shear without buckling, resin stiffness has no effect.

Fibers having a higher tensile failure strain are seen to buckle at a higher strain (Fig. 12). The P75 fiber is weaker in compression than in tension. However, both T300 and T700 fibers are stronger in compression. The E-glass fiber is slightly weaker in compression.

Buckling of a single fiber embedded in a matrix has been analyzed in the literature.[11-13] The approximate analysis in Ref. 13 indicates that the buckling strain ε_b and buckle wavelength λ of the fiber are related to the moduli E_m, E_f and the fiber diameter d_f by

$$\varepsilon_b \propto (E_m/E_f)^{1/2} \tag{1}$$

$$\lambda \propto (E_f/E_m)^{1/4}\, d_f \tag{2}$$

where subscripts m and f denote matrix and fiber, respectively.

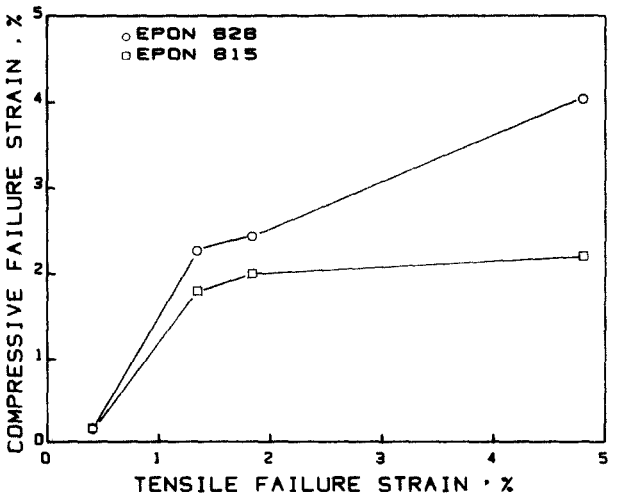

Fig. 12. Compressive failure strain increasing with tensile failure strain.

Figures 13 and 14 show that the present data follow the trends predicted by eqns (1) and (2), although a bundle of fibers rather than a single fiber was used. In Fig. 13 the buckling strains of T300, T700, and E-glass are seen to be proportional to the square root of the matrix-to-fiber modulus ratio. The failure strains of P75 are not supposed to be on the line since the failure was by shear and not by microbuckling. In Fig. 14

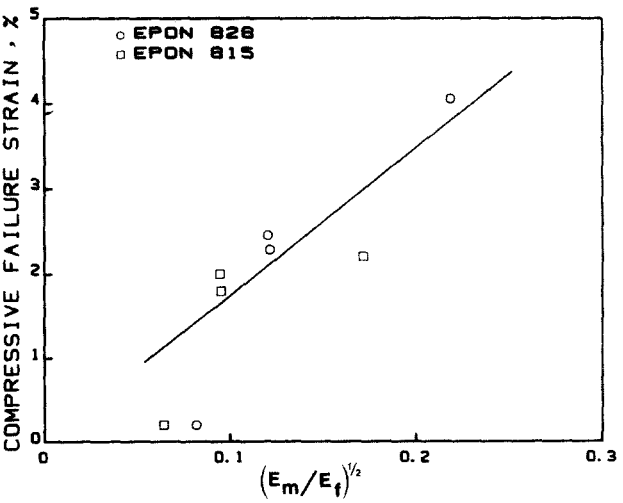

Fig. 13. Compressive failure strain increasing with square root of matrix-to-fiber modulus ratio.

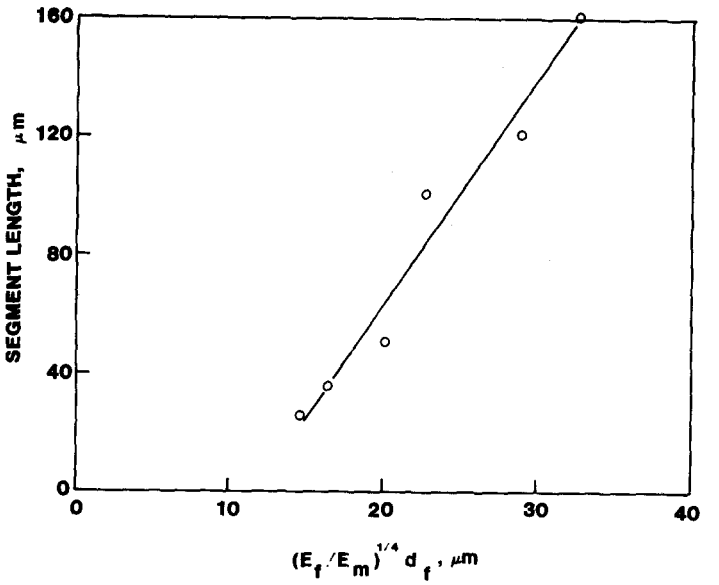

Fig. 14. Average segment length increasing with quadratic root of fiber-to-matrix modulus ratio and with fiber diameter.

the segment length increases linearly with fiber diameter and with the quadratic root of the fiber-to-matrix modulus ratio, although the relationship does not go through the origin. It is, however, worthwhile to take a new look at the theory, possibly taking into account the evidence that the yield stress and the tensile fracture stress of the matrix and the interface play a role in determining compressive failure under appropriate conditions, rather than the matrix modulus.[14]

CONCLUSIONS

The use of a fiber bundle embedded in resin can provide much needed information on compressive failure mechanisms in unidirectional composites because failure of the bundle is well contained and can be monitored during testing. The method can clearly distinguish between buckling-induced failure and shear-induced failure of fibers. The present study indicates that the T300 and T700 graphite fibers and the E-glass fibers fail in buckling, while the high-modulus P75 fibers fail in shear. Buckling-induced failure is most evident for the E-glass fibers, while the

kinking type of failure is common for the T300 and T700 graphite fibers. Further specific conclusions are as follows:

1. Buckling of fibers is uniformly distributed in a very soft resin, but quite localized in stiff resins.
2. Fiber fracture occurs immediately after buckling. Debonding also follows fiber buckling.
3. Observed failure strains and segment lengths of the bundle specimens follow the trends predicted for a single fiber embedded in an infinite matrix.
4. With the exception of the P75 graphite, compressive failure strains of the fibers studied are higher than those of their composites. Thus, compressive strengths of the fibers are not fully utilized in composites.

ACKNOWLEDGEMENTS

The present paper is based on work supported by NASA Langley Research Center under Grant NAG-1-295 with J. G. Williams as the Project Engineer. The authors wish to thank T. Johannesson for SEM work, and J. F. Kay of Owens/Corning Fiberglas and M. K. Towne of Union Carbide Corp., for supplying E-glass and graphite fibers, respectively.

REFERENCES

1. J. G. Williams and M. D. Rhodes, Effect of resin on impact damage tolerance of graphite/epoxy laminates, in: *Composite Materials: Testing and Design (Sixth Conf.)*, (Ed. I. M. Daniel), ASTM-STP 787, Philadelphia, USA, 1982, pp. 450–80.
2. N. Hancox, The compression strength of unidirectional carbon fibre reinforced plastic, *J. Mater. Sci.*, **10** (1975), pp. 234–42.
3. L. B. Greszczuk, On failure modes of unidirectional composites under compressive loading, in: *Proc. of 2nd USA–USSR Symp. on Fracture of Composite Materials* (Ed. G. C. Sih), Martinus Nijhoff Publishers, The Hague, 1981, pp. 231–46.
4. C. W. Weaver and J. G. Williams, Deformation of a carbon–epoxy composite under hydrostatic pressure, *J. Mater. Sci.*, **10** (1975), pp. 1323–33.
5. C. R. Chaplin, Compressive fracture in unidirectional glass-reinforced plastics, *J. Mater. Sci.*, **12** (1977), pp. 347–52.

6. A. G. Evans and W. F. Adler, Kinking as a mode of structural degradation in carbon fiber composites, *Acta Met.*, **26** (1978), pp. 725–38.
7. S. V. Kulkarni, J. R. Rice and B. W. Rosen, An investigation of the compressive strength of Kevlar 49/epoxy composites, *Composites*, **6** (1975), pp. 217–25.
8. H. T. Hahn and J. G. Williams, Compression failure mechanisms in unidirectional composites, paper presented at the ASTM Symp. on Composite Materials: Testing and Design (Seventh Conf.), Philadelphia, USA, 1984.
9. H. M. Hawthorne and E. Teghtsoonian, Axial compression fracture in carbon fibers, *J. Mater. Sci.*, **10** (1975), pp. 41–51.
10. L. Lorenzo and H. T. Hahn, Acoustic emission study of fracture of fibers embedded in epoxy matrix, in: *Proc. First Int. Symp. on Acoustic Emission from Reinforced Composites*, SPI, 1983, Session 2.
11. M. A. Sadowsky, S. L. Pu and M. A. Hussain, Buckling of microfibers, *J. Appl. Mech.*, **34** (1967), pp. 1011–16.
12. L. R. Herrmann, W. E. Mason and T. K. Chan, Response of reinforcing wires to compressive states of stress, *J. Comp. Mater.*, **1** (1967), pp. 212–26.
13. Y. Lanir and Y. C. B. Fung, Fiber composite columns under compression, *J. Comp. Mater.*, **6** (1972), pp. 387–401.
14. M. R. Piggott, A theoretical framework for the compressive properties of aligned fiber composites, *J. Mater. Sci.*, **16** (1981), pp. 2837–45.